

RESEARCH ARTICLE

10.1029/2018JG004875

Key Points:

- Mangrove-estuary exchange of nitrogen was mainly driven by tidal pumping
- Mangrove sediments mostly serve as ammonium source but nitrate sink
- Strong mineralization leads to accumulation of ammonium in pore water, while denitrification dominates nitrate removal and N₂O production

Supporting Information:

- Supporting Information S1

Correspondence to:

N. Chen,
nwchen@xmu.edu.cn

Citation:

Wang, F., Chen, N., Yan, J., Lin, J., Guo, W., Cheng, P., et al. (2019). Major processes shaping mangroves as inorganic nitrogen sources or sinks: Insights from a multidisciplinary study. *Journal of Geophysical Research: Biogeosciences*, 124. <https://doi.org/10.1029/2018JG004875>

Received 17 DEC 2018

Accepted 30 MAR 2019

Accepted article online 10 APR 2019

Author Contributions:

Conceptualization: Nengwang Chen**Data curation:** Nengwang Chen**Formal analysis:** Nengwang Chen**Funding acquisition:** Nengwang Chen**Investigation:** Nengwang Chen**Methodology:** Nengwang Chen**Project administration:** Nengwang Chen**Resources:** Nengwang Chen**Software:** Nengwang Chen**Supervision:** Nengwang Chen**Validation:** Nengwang Chen**Visualization:** Nengwang Chen**Writing - original draft:** Nengwang Chen**Writing - review & editing:** Nengwang Chen

Major Processes Shaping Mangroves as Inorganic Nitrogen Sources or Sinks: Insights From a Multidisciplinary Study

Fenfang Wang¹, Nengwang Chen^{1,2} , Jing Yan¹, Jingjie Lin¹, Weidong Guo² , Peng Cheng² , Qian Liu^{2,3}, Bangqin Huang^{1,2} , and Yun Tian^{1,4}

¹Key Laboratory of the Coastal and Wetland Ecosystems, College of the Environment and Ecology, Xiamen University, Xiamen, China, ²State Key Laboratory of Marine Environment Science, Xiamen University, Xiamen, China, ³Key Laboratory of Marine Chemistry Theory and Technology, Ministry Education, Ocean University of China, Qingdao, China, ⁴School of Life Science, Xiamen University, Xiamen, China

Abstract Mangrove wetlands support numerous ecosystem services including nutrient cycling and carbon sequestration and storage (blue carbon). Mangrove sediments may serve as a nitrogen source or sink to the hydrosphere and atmosphere at both regional and global scales. However, major mechanisms controlling the connection between the mangrove and the adjacent tidal creek (nitrogen cycling in sediments and outfluxing) remain unclear. A multidisciplinary study based on intensive investigation, incorporating detailed sediment profiling, multi-isotopes analysis, sediment incubation, and microbiological identification was conducted in the Yunxiao mangrove reserve and Zhangjiang Estuary in southeast China. Here we show that mineralization and denitrification are major processes shaping mangroves as an ammonium source and nitrate sink. Enrichment of ammonium in pore water (10–40 cm in depth) likely resulted from strong ammonification with limited nitrification in the anaerobic sediments. Denitrification played a key role in nitrate removal from pore waters while producing N₂O and N₂. Decreasing δ¹⁵N-N₂O and associated δ¹⁵N:δ¹⁸O ratio suggested that most of the outgassing N₂O was derived from incomplete denitrification in sediment pore water. Overall, there was a net export of dissolved inorganic nitrogen from mangroves toward the estuary in winter and spring but a net import to mangroves in summer and fall, mainly driven by tidal pumping with seasonal variation of bio-uptake. These findings highlight the role of mangrove wetlands in regulating nutrient status and carbon budget in coastal areas.

1. Introduction

Mangrove forests stretching along tropical and subtropical coastlines provide a wealth of ecosystem services, including fisheries production, nutrient cycling, and carbon sequestration at local, regional, and global scales (Rivera-Monroy et al., 2017). Over the past decades, mangrove ecosystems across the globe have been lost or degraded due to various human activities and climate change impacts (Alongi, 2015; Gilman et al., 2008). Nitrogen and phosphorus are critical nutrients that mediate mangrove forest productivity and structural properties (Feller et al., 2010; Lovelock et al., 2009; Reef et al., 2010). Nutrient cycling regulates the role of mangroves in carbon sequestration and carbon storage (so-called blue carbon), which has recently been considered as a potential mitigation measure to climate change (McLeod et al., 2011). For example, nutrient consumption and regeneration have a great impact on mangrove productivity and organic matter mineralization (Lee et al., 2008). Eutrophic mangrove systems receiving high nutrient loads may accumulate much more organic matter than undisturbed ones (Sanders et al., 2014). Organic stocks differ along the land-to-sea gradient resulting from nutrient limitation (Weiss et al., 2016). Although the value of and threats to mangroves have been well recognized, studies on the coupled nutrient and carbon biogeochemistry bridging terrestrial and aquatic realms are limited. Such knowledge gaps have limited our ability to properly restore degraded ecosystems and achieve sustainable development in the context of increased anthropogenic pressures and climate perturbation.

A few studies on nutrient dynamics in tidal creeks reveal that mangrove forests can be either a nitrogen source or sink, varying with nitrogen forms (inorganic or organic and dissolved or particulate) and seasons (Dittmar & Lara, 2001a; Rivera-Monroy et al., 1995; Sánchez-Carrillo & Sánchez-Andrés, 2009; Valiela et al.,

2018). A number of probable factors (e.g., litterfall, sediment, nitrogen demands by plants, climate, and river runoff) have been used to explain creek water nitrogen dynamic and fluxes (Chen & Twilley, 1999; Dittmar, 1999; Inoue et al., 2011; Mandal et al., 2013). Mangrove pore water exchange has been recently found to release nitrogen into estuarine water due to the complex belowground structure of crab burrows and the effect of tidal pumping (Sadat-Noori et al., 2017). Exchange rates between seawater and groundwater over the tidal cycle have been estimated to analyze its effect on nitrogen transformation (Xiao et al., 2018). Insight into sediment nitrogen cycling processes is essential to understand the interactions between mangrove wetlands and the adjacent waters. However, sediment metabolism and pore water biogeochemistry are rarely investigated (Lee et al., 2008).

Nitrogen isotope tracer techniques have been widely used to quantify nitrogen transformations in sediments (Kristensen et al., 1998; Reis et al., 2017; Rivera-Monroy & Twilley, 1996). However, analysis of stable multi-isotopes of nitrogen forms (e.g., ^{15}N and ^{18}O of nitrate, ammonium, and N_2O) is rarely applied to define nitrogen source and cycling processes involved in the mangrove system. Furthermore, nitrogen biogeochemistry is mostly microbe driven, but microbiological identification is rarely incorporated into biogeochemical studies of mangrove systems (Amano et al., 2011; Li & Gu, 2013; Wang et al., 2014). Given that mangrove nitrogen biogeochemistry is diverse over time and space, a multidisciplinary approach is vital to reveal the underlying mechanisms and major processes controlling nitrogen cycling and outwelling across mangrove wetlands to hydrosphere and atmosphere.

Mangrove forests in China fringe many subtropical estuaries and islands. They have experienced major disturbance from agriculture, aquaculture, and urbanization. In 2016, the Yunxiao National Mangrove Nature Reserve and the adjacent Zhangjiang Estuary in Fujian province (southeast China) were selected as a blue carbon pilot study site. The mangrove receives upstream effluents (e.g., sewage and aquaculture pond drainage), which discharge through a few sluices during low-tide periods. As an initial stage of research efforts toward understanding how the mangrove ecosystem is responding to a changing environment, this study focuses on nitrogen. Here we report the results of a multidisciplinary study based on an intensive investigation across the mangrove-creek-estuary continuum, including time series measurement of creek water with multi-isotopes analysis, detailed sediment profiling, sediment incubation, and microbiological identification. The specific objectives of this study were (1) to characterize seasonal and spatial variation of nitrogen forms ($\text{NH}_4\text{-N}$, $\text{NO}_2\text{-N}$, and $\text{NO}_3\text{-N}$) from mangrove through tidal creek to adjacent estuary; (2) to explore temporal dynamics of nitrogen with isotope signatures ($\delta^{15}\text{N}\delta^{18}\text{O}_3^-$, $\delta^{15}\text{NH}_4^+$, and $\delta^{15}\text{N}_2\delta^{18}\text{O}$), dissolved N_2 , and N_2O during ebb tide and low tide; and (3) to quantify the nitrogen transformation down to sediment profiles using a stoichiometry-based incubation approach. The comprehensive data set we obtained was then used to examine the hydrobiogeochemical controls on nitrogen cycling and exchange between the mangrove and tidal creek and to further reveal major processes shaping mangroves as a dissolved inorganic nitrogen (DIN) source or sink.

2. Materials and Methods

2.1. Description of Study Site

The study was conducted at Yunxiao National Mangrove Reserve and Zhangjiang estuary in Southeast China (Figure 1). The dominant species in the mangrove forest are *Avicennia marina*, *Kandelia candel*, and *Aegiceras corniculatum* (Zhou et al., 2010). The study area experiences a subtropical monsoon climate. The climatic factors show obvious seasonal dynamics (Figure S1 in the supporting information). Air temperature in spring (March–May), summer (June–August), fall (September–November), and winter (December–February) is 14.8–21.7 °C, 25.6–29.1 °C, 25.9–29.6 °C, and 14.8–16.6 °C, respectively, with an annual mean temperature of 22.8 °C. Monthly precipitation varies from 1 to 404 mm with an annual precipitation of 1,679 mm. The largest precipitation occurred in summer (1,030 mm), and the precipitation in fall and winter is much smaller (187 and 91 mm). The solar radiation in summer and fall (1,802 and 1,666 MJ) is much higher than spring and winter (1,520 and 1,403 MJ). Wind speed is 1.87–3.13 m/s between January and October and reaches 16.64 and 17.21 m/s in November and December. The estuary has a semidiurnal tide with a large range (0.43–4.67 m). Land uses in the upstream area include residential land, cropland, and aquaculture ponds that produce domestic wastewater, agricultural runoff, and aquaculture effluents.

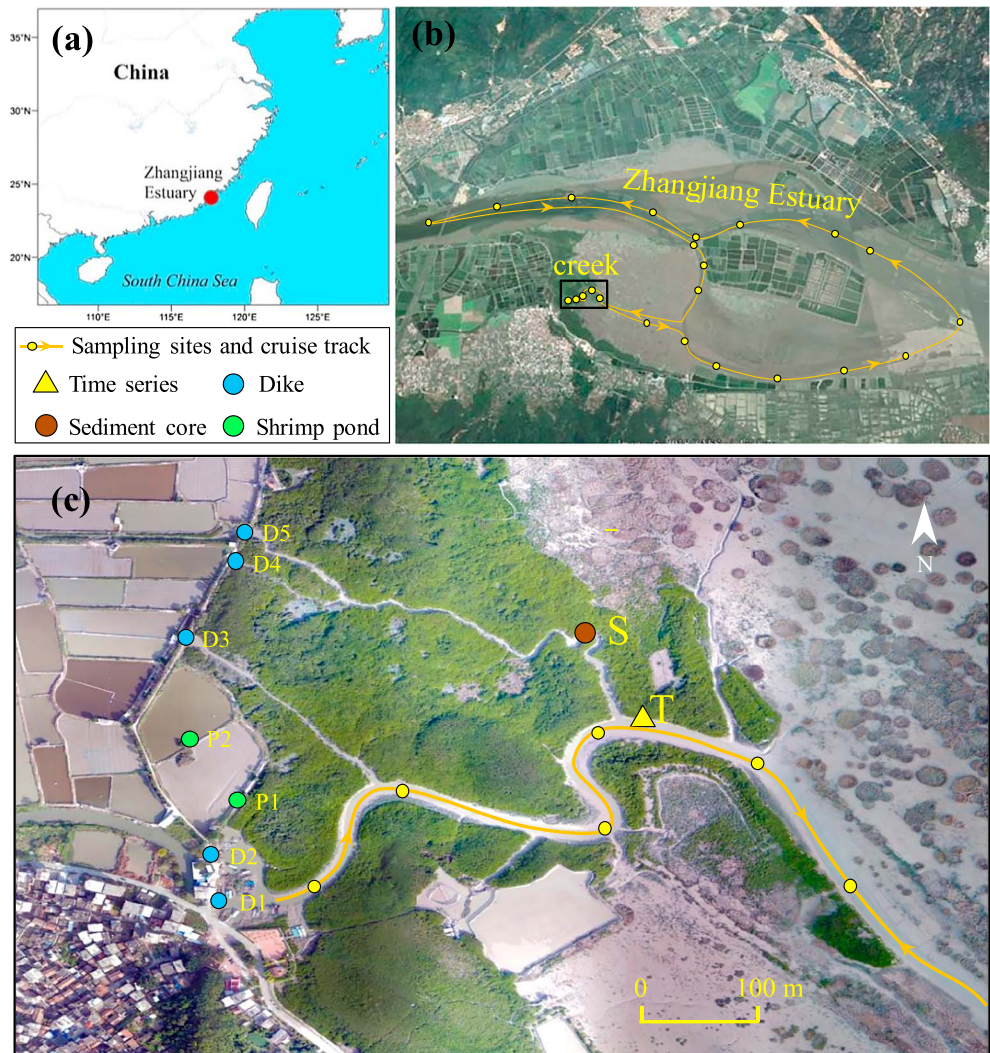


Figure 1. Map of study area showing sampling sites along tidal creek and Zhangjiang Estuary; arrows on the line indicate cruise track direction (b). D1-D5 in (c) are the locations of dikes discharging effluents to tidal creek. P1 and P2 are shrimp ponds. Time series measurements (site T) were performed at the middle of tidal creek, and sediment cores (site S) were collected at the mangrove forest margin of tidal creek, Yunxiao, Fujian, China (a).

2.2. Sampling Campaign

The study targeted the mangrove-tidal creek-estuary continuum. We collected water samples from the upstream effluent area through the major tidal creek to adjacent estuary (Figure 1b). In the tidal creek, water samples were collected during both flood and ebb tide to compare the concentrations of nutrients in the mangrove zone and estuarine water. Five cruises were conducted on 13 January (winter), 26 March (spring), 28 April (spring), 22 June (summer), and 31 October (fall) 2017 to understand the seasonal variation. Surface water samples were collected using a Niskin hydrophore and were stored in polyethylene bottles at 4 °C.

A fixed site at the lower mangrove tidal creek (site T) was chosen to conduct time series measurements on 28 April 2017 (Figure 1c). Hourly measurements last 25 hr, but we mainly used the results during ebb and low tide to identify the influence of sediment pore water and upstream effluent discharge on creek water. Time series samples were analyzed for nutrient concentrations, isotopic compositions, and dissolved gases (N_2 and N_2O). Water for dissolved gases analysis was introduced into the bottom of 12- (N_2) and 60-ml (N_2O) glass bottles through a silicone tube. After about 3+ volumes of water had overflowed from the bottle, a final concentration of 0.1% of $HgCl_2$ was added to stop microbial activity. The bottles were immediately capped without air space and stored in a cooler containing fresh water to maintain temperature.

Dissolved oxygen (DO), temperature, pH, and salinity were measured in situ using a multiparameter portable meter (WTW 3430, Germany). Water depth at fixed site T was continuously recorded by a Sea-Sun Tech CTD 48M probe.

To investigate nitrogen cycling processes within sediments, sediment cores were collected using a plexiglass pipe ($\Phi 120$ mm \times 500 mm) from the side slope of a tributary creek (site S; Figure 1c). Sediment cores were sampled in April, June, and December 2017. Sediment cores for incubation were collected in December 2017. All sediment samples were stored at 4 °C before transported to the laboratory for physicochemical analysis and incubation. One more sediment core was prepared for molecular analysis (N functional genes) in June 2017 at the same site.

2.3. Laboratory Analysis

A total of 50-ml water was filtered in the field by a GF/F membrane and refrigerated at 4 °C until analysis within 2 days. Filtrate was used to measure dissolved nutrient forms, that is, nitrate ($\text{NO}_3\text{-N}$), nitrite ($\text{NO}_2\text{-N}$), ammonium ($\text{NH}_4\text{-N}$), and total dissolved nitrogen (TDN). $\text{NO}_3\text{-N}$, $\text{NO}_2\text{-N}$, and $\text{NH}_4\text{-N}$ were analyzed by segmented flow automated colorimetry (San++ analyzer, Germany). TDN concentrations were determined as $\text{NO}_3\text{-N}$ following oxidization with 4% alkaline potassium persulfate. DIN is the sum of $\text{NO}_3\text{-N}$, $\text{NO}_2\text{-N}$, and $\text{NH}_4\text{-N}$. Dissolved organic nitrogen (DON) was the difference between TDN and DIN.

Dissolved N_2 concentrations were measured using the $\text{N}_2\text{-Ar}$ method by a membrane inlet mass spectrometry system (Chen et al., 2014). The concentrations of N_2O were measured by a Gas Chromatograph (Agilent 7890A, U.S.). Isotopic analysis of nitrate was conducted by a denitrifier method (Casciotti et al., 2002; Sigman et al., 2001), in which nitrate was reduced to N_2O by denitrifying bacteria that lack N_2O -reductase activity, and isotopic compositions were measured by an isotope ratio mass spectrometer (Isoprime 100, UK). $\delta^{15}\text{N-NH}_4^+$ was measured with ammonia diffusion method (Holmes et al., 1998). $\delta^{15}\text{N}$ and $\delta^{18}\text{O}$ analysis of dissolved N_2O was carried out using a trace gas preparation unit (Precon, Finnigan, Germany) coupled to an isotope ratio mass spectrometer (Delta V, Finnigan, Germany). The details of the analyses, detection limits, and calibration are shown in the supporting information (SI) section.

The sediment core was sectioned into intervals of 1–5-cm thickness before extraction and analysis of pore water and solid-phase constituents. Sediment of each depth was homogenized and transferred to 50-ml polypropylene centrifuge tubes and then centrifuged at 4,500 rpm for 20 min. The supernatant of pore water was filtered over 0.45- μm Teflon filters before analysis of $\text{NO}_3\text{-N}$, $\text{NO}_2\text{-N}$, and $\text{NH}_4\text{-N}$. Chromophoric dissolved organic matter (CDOM) abundance was quantified by the absorption coefficient at the wavelength of 350 nm ($a_{\text{CDOM}}(350)$). The absorption spectra were determined by a 2300 UV-Visible spectrophotometer (Techcomp, China; Guo et al., 2014). DOC and DIC concentrations were determined by TOC-VCPH analyzer and LI 7000 $\text{CO}_2/\text{H}_2\text{O}$ analyzer, respectively. A subsample of sediment was transferred into 15-ml preweighed glass vials and was freeze-dried. The dried sediment was prepared with 1:5 water-to-sediment ratio to measure pH and Eh using a WTW multiparameter meter (Multi 3430, Germany). A subsample of dried sediment was ground and acidified with 1-M HCl to determine the content of total organic carbon (POC) and total nitrogen (TN) by an element analyzer (PE2400 SERIES IICHNS/O).

For molecular analysis, triplicate sediment samples were selected at depth of 1 (surface), 17 (middle), and 33 cm (bottom). DNA was extracted from approximately 0.5-g sediment using a Fast DNA Spin Kit for Soil, suspended in 50- μL TE solution and stored at -80 °C until analysis. All DNA were quantified by a Nano Drop spectrophotometer (DN-1000; Isogen Life Science, the Netherlands). Ammonia-oxidizing archaea (AOA) and ammonia-oxidizing bacteria (AOB) were quantified by a Bio-Rad CFX96 qPCR. The diversity of AOA and AOB was determined by cloning and sequencing of PCR-amplified *amoA* genes, using primers Arch-*amoA*F and Arch-*amoA*R for AOA (Francis et al., 2005) and *amoA*-1F and *amoA*-2R for AOB (Wang et al., 2011). The nitrous oxide reductase gene (*nosZ*) was determined by cloning and primers of PCR-amplified gene CAMP-*Nos661F* and CAMP-*Nos1773R* (Scala & Kerkhof, 1999).

2.4. Data Analysis and Statistics

The dissolved N_2 in water is produced by biological (mainly denitrification) and physical processes, while Ar is just influenced by physical factors, so the ratio of N_2 to Ar can be used to precisely quantify the production

Table 1
Nitrogen Concentration and Fraction of TDN (Mean ± SD) Across the Upstream Effluent, Tidal Creek, and Estuary

Sampling date	Sample group	NH ₄ -N (μmol/L)	NO ₃ -N (μmol/L)	NO ₂ -N (μmol/L)	DON (μmol/L)	NH ₄ -N (%)	NO ₃ -N (%)	NO ₂ -N (%)	DON (%)
13 January 2017	tidal creek-flood	28.7 ± 6.8	154.5 ± 13.6	9.1 ± 1.2	35.8 ± 3.9	12 ± 2	68 ± 1	4 ± 0.2	16 ± 3
	tidal creek-ebb	50.8 ± 13.7	170.6 ± 3.7	10.6 ± 2.6	34.2 ± 5.0	19 ± 5	64 ± 3	4 ± 1	13 ± 2
	estuary	23.7 ± 10.0	150.8 ± 51.0	7.7 ± 2.4	33.8 ± 7.0	11 ± 2	69 ± 3	4 ± 0.4	17 ± 4
26 March 2017	tidal creek-flood	30.4 ± 12.1	104.8 ± 4.5	11.1 ± 1.7	49.5 ± 6.7	15 ± 5	54 ± 4	6 ± 0.4	25 ± 4
	tidal creek-ebb	53.5 ± 16.3	108.9 ± 3.1	14.1 ± 2.9	50.0 ± 4.9	24 ± 6	48 ± 5	6 ± 1	22 ± 3
	estuary	33.7 ± 24.3	113.3 ± 40.1	11.0 ± 4.1	48.6 ± 6.8	14 ± 7	55 ± 2	5 ± 1	26 ± 9
28 April 2017	tidal creek-flood	73.1 ± 47.8	175.5 ± 36.2	14.9 ± 1.6	67.3 ± 14.0	21 ± 7	54 ± 5	5 ± 1	21 ± 2
	tidal creek-ebb	106.9 ± 15.2	195.2 ± 11.6	17.1 ± 0.7	69.8 ± 29.5	28 ± 4	51 ± 3	4 ± 0.3	18 ± 7
	estuary	37.9 ± 14.2	132.2 ± 45.6	11.5 ± 3.3	71.5 ± 15.0	15 ± 2	51 ± 5	5 ± 1	30 ± 7
22 June 2017	tidal creek-flood	28.9 ± 2.0	231.1 ± 13.2	9.4 ± 0.2	9.9 ± 12.0	10 ± 0.3	83 ± 4	3 ± 0.2	4 ± 4
	tidal creek-ebb	31.0 ± 1.9	201.5 ± 11.8	10.5 ± 0.5	13.6 ± 7.9	12 ± 1	79 ± 4	4 ± 0.2	5 ± 3
	estuary	23.4 ± 3.8	198.3 ± 52.8	8.2 ± 1.8	6.9 ± 7.1	10 ± 2	83 ± 3	3 ± 0.3	3 ± 3
31 October 2017	tidal creek-flood	18.6 ± 2.9	88.9 ± 2.7	10.0 ± 0.2	19.0 ± 6.9	14 ± 1	65 ± 5	7 ± 0.4	14 ± 4
	tidal creek-ebb	16.6 ± 4.7	80.2 ± 5.4	8.4 ± 0.9	26.3 ± 2.8	12 ± 3	60 ± 3	7 ± 0.5	20 ± 2
	estuary	22.7 ± 7.2	140.6 ± 23.3	12.0 ± 1.5	19.0 ± 9.1	13 ± 2	69 ± 2	7 ± 1	10 ± 3
Average, 2017	tidal creek-flood	35.9 ± 21.3	151.0 ± 57.1	10.9 ± 2.4	36.3 ± 23.1	14 ± 4	65 ± 12	5 ± 2	16 ± 8
	tidal creek-ebb	52.0 ± 34.0	151.2 ± 54.2	12.2 ± 3.3	38.4 ± 22.0	19 ± 7	61 ± 12	5 ± 1	15 ± 6
	estuary	28.3 ± 7.0	147.0 ± 31.8	10.1 ± 2.0	36.0 ± 25.3	13 ± 2	65 ± 13	5 ± 1	17 ± 11
13 December 2017	sluice effluent and pond water	175.5 ± 79.1	72.8 ± 9.7	16.4 ± 4.0	18.2 ± 10.4	59 ± 13	27 ± 9	6 ± 1	7 ± 5

of N₂. Net denitrification product (excess N₂ or ΔN₂) was calculated with equation (1). See more details in our previous study (Chen et al., 2014).

$$\Delta N_2 = [N_2 : Ar]_{\text{measured}} * [Ar]_{\text{expected}} - [N_2]_{\text{expected}} \quad (1)$$

where ΔN₂ is the net N₂ production. Positive and negative values signify net denitrification and net nitrogen fixation, respectively. [N₂:Ar]_{measured} is the measured concentration (μmol/L) ratio of N₂:Ar that have been calibrated using air-equilibrated water standards; [Ar]_{expected} and [N₂]_{expected} are the concentrations when the water was in equilibrium with the atmosphere and is derived by Weiss (1970).

The excess production of N₂O (ΔN₂O) was calculated with the equation (2). See more details in our previous study (Chen et al., 2015).

$$\Delta N_2O = N_2O_{(\text{water})} - N_2O_{(\text{eq})} \quad (2)$$

where N₂O_(water) is measured concentration of dissolved N₂O (nmol/L) in water; N₂O_(eq) is the concentration when the water was in equilibrium with the atmosphere and is derived by Weiss and Price (1980).

Regression analyses were conducted to obtain the relationship between tidal range and nitrogen offset in ebb tide from the mixing line of estuary. Group T-test was conducted to test the difference of δ¹⁵N between ebb tide and low tide (the effluent affected period). Chi-square test was operated to see whether there was an increased or decreased trend for nitrogen concentrations and dissolved gases during ebb tide. All the statistical analyses were performed using SPSS 19.0 software package.

2.5. Sediment Incubation

A sediment core was sectioned into intervals of 5-cm thickness. For each layer, sediment slurry was homogenized in field with water (4:3 ratio of water to sediment). An 8-ml slurry was transferred into 60-ml brown glass bottles using a 10-ml syringe. The bottles were filled with filtered in situ water till overflowing and closed. Another bottle with filtered water only was used as a control. After incubation for 60 hr, nutrients and dissolved gases (N₂ and N₂O) in the supernatant were measured as described above. The increase in final concentration of sediment samples and controls was considered as the net production by sediment during incubation. The transformation of nitrogen forms was determined as change in their concentrations over time by subtracting initial from final values after incubation. DO was not controlled during incubation but was expected to consume gradually, simulating the change from oxic/suboxic (emergence) to anaerobic condition (inundation) across a tidal cycle.

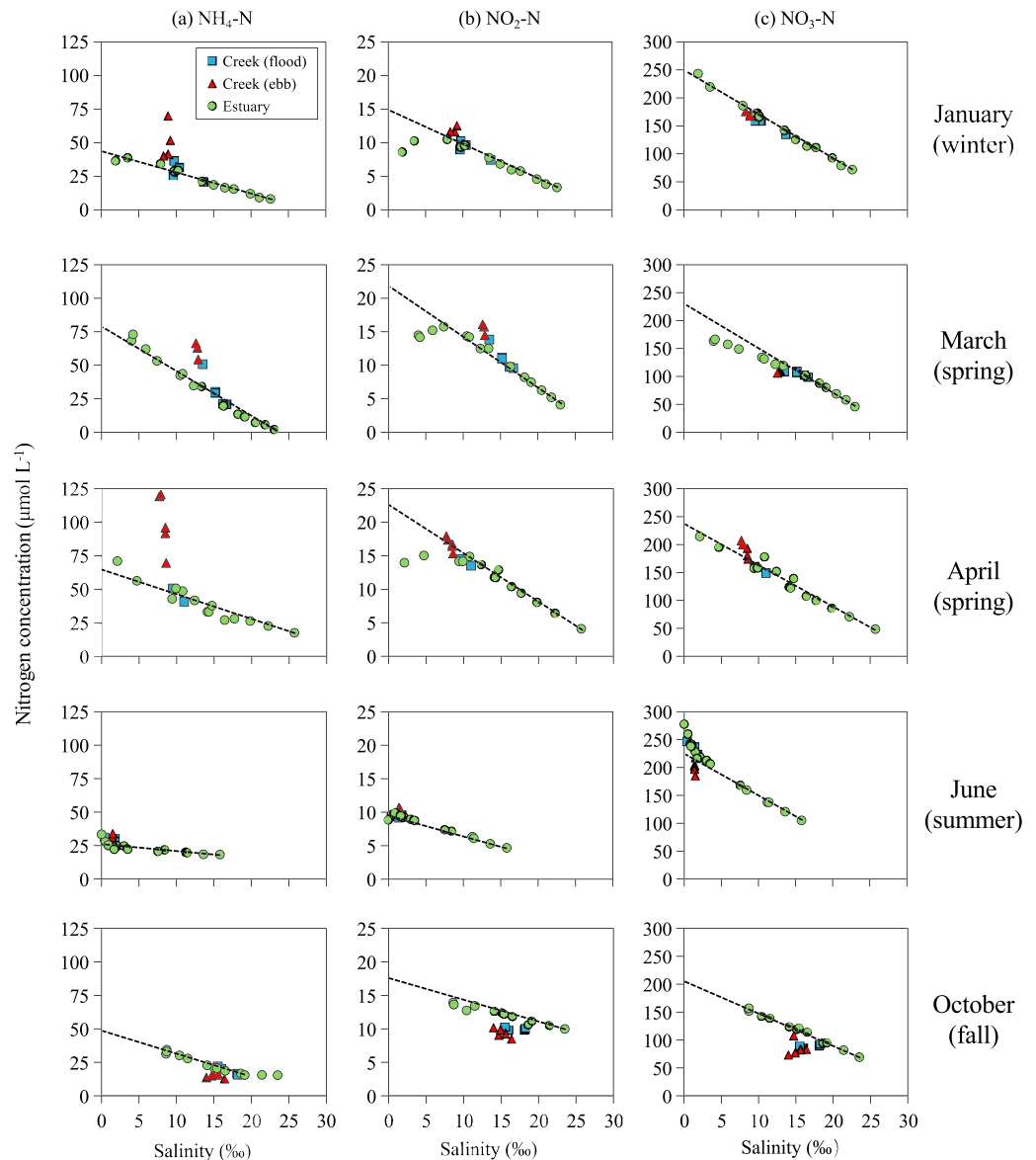


Figure 2. Diagram of measured nitrogen concentration against salinity (2017). Squares and triangles indicate the creek water samples during flood and ebb tide, respectively. The dotted regression lines indicate conservative mixing along the higher salinity gradient. The samples with lower salinity at upstream were not included in the regression line.

3. Results

3.1. Spatial and Temporal Variation of Nitrogen Concentrations and Compositions

Nitrogen concentrations and compositions differed between the sluice effluents (and aquaculture ponds), the tidal creek, and the estuary (Table 1). Simple unweighted average $\text{NH}_4\text{-N}$ concentration and the fraction of TDN in the tidal creek ($44.0 \mu\text{mol/L}$ and 17%) were higher than in the estuary ($28.3 \mu\text{mol/L}$ and 13%). Likewise, average $\text{NO}_3\text{-N}$ ($151.1 \mu\text{mol/L}$ and 63%) in the creek was somewhat higher than in the estuary ($147.0 \mu\text{mol/L}$ and 65%) with an exception in April. Compared to creek and estuary water, upper stream effluent had a much higher $\text{NH}_4\text{-N}$ concentration ($175.5 \mu\text{mol/L}$) and fraction (59%) but lower $\text{NO}_3\text{-N}$ concentration ($72.8 \mu\text{mol/L}$) and fraction (27%). Overall, DIN was the major form (70%–97%) of dissolved nitrogen across seasons.

In the tidal creek, nitrogen concentrations across tidal cycles (flood versus ebb tide) and seasons showed a distinct temporal variation (Table 1). Average $\text{NH}_4\text{-N}$ and DON in ebb tide (52.0 and $38.4 \mu\text{mol/L}$) were

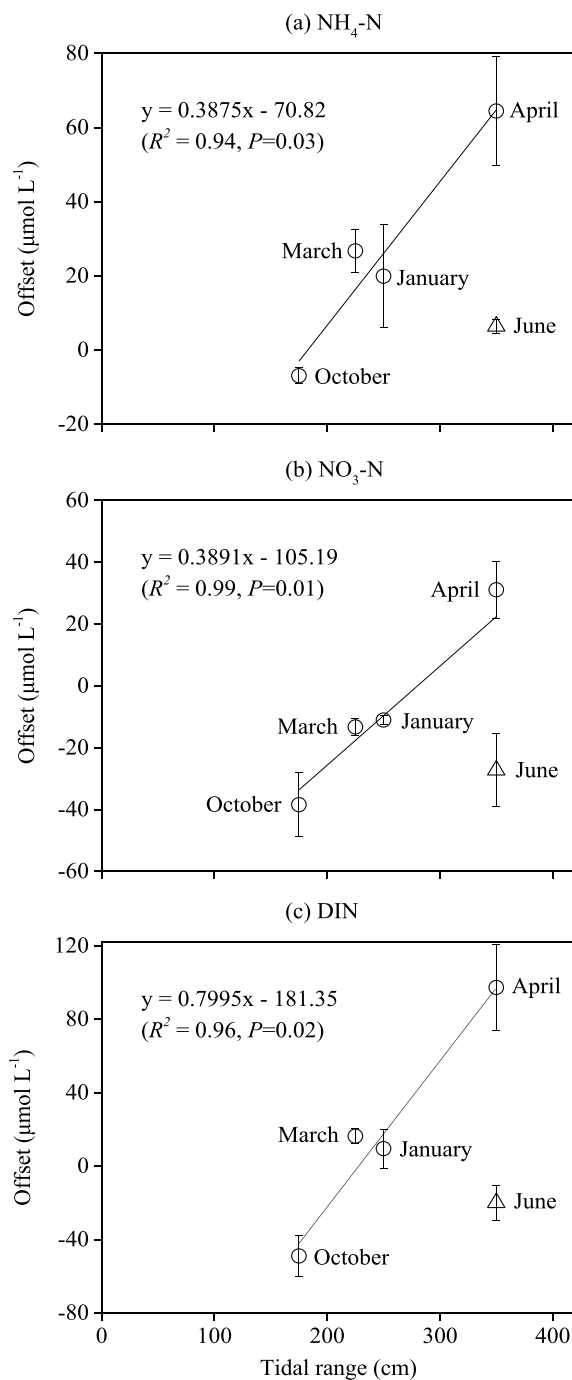


Figure 3. Relationship between tidal range and nitrogen offset in ebb tide from mixing line of estuary (refer to Figure 2). The results in June (triangles) were not included in the linear regression of nitrogen offset against tidal range. The offset of $\text{NH}_4\text{-N}$, $\text{NO}_3\text{-N}$, and DIN were indicated by (a), (b), and (c).

nitrate were between 1.0 and 2.1, which reflects the denitrification process involved (Amberger & Schmidt, 1987).

3.3. Profile of Sediment Physicochemistry and Functional Gene Abundance

Water content in sediments was low (40%–55%), and there was no obvious change along the profile (Figure 6a). Sediment Eh was fairly low (–80–20 mV), and a minimum value was found in top sediments

higher than flood tide (35.9 and 36.3 $\mu\text{mol/L}$), but $\text{NO}_3\text{-N}$ (151.2 $\mu\text{mol/L}$) was almost the same level as flood tide (151.0 $\mu\text{mol/L}$). The average concentrations of $\text{NH}_4\text{-N}$, $\text{NO}_3\text{-N}$, and $\text{NO}_2\text{-N}$ in autumn (October) were among the lowest compared to other seasons. $\text{NH}_4\text{-N}$ (30.0 $\mu\text{mol/L}$) in summer (June) was lower than spring (March and April; 66.0 $\mu\text{mol/L}$) and winter (January; 39.8 $\mu\text{mol/L}$), while $\text{NO}_3\text{-N}$ (216.3 $\mu\text{mol/L}$) was among the highest in summer.

Nitrogen-salinity diagrams showed that nitrogen behavior was mostly conservative along the river estuary gradient for the high-salinity region. Nitrogen concentrations in tidal creek had more or less offset from the estuary (i.e., concentration deviation from the regression line of estuarine data points; Figure 2). In a given salinity, $\text{NH}_4\text{-N}$ in the creek was always greater than in the estuary during ebb tide except in October, while $\text{NO}_3\text{-N}$ in creek was generally lower than in the estuary. DIN showed positive offset in winter and spring but negative offset in summer and fall (Figure 3). Salinity in the tidal creek in June (0.4‰–2.1‰) was much lower than the other four months (6.4‰–18.2‰; Figure 2). There were strong positive correlations between tidal range and the offset of $\text{NH}_4\text{-N}$ ($R^2 = 0.94$, $P = 0.03$), $\text{NO}_3\text{-N}$ ($R^2 = 0.99$, $P = 0.01$), and DIN ($R^2 = 0.96$, $P = 0.02$) in ebb tide, with the exception of the June cruise, which was conducted immediately after a rain storm (Figure 3).

3.2. Time Series of Nitrogen Concentrations, Isotopic Compositions, and Dissolved Gases in the Tidal Creek

The nitrogen concentrations, isotopic compositions, and dissolved gases changed gradually with the decreasing water depth during ebb tide but fluctuated at low tide (Figure 4). During ebb tide, $\text{NO}_3\text{-N}$ changed little, while $\text{NH}_4\text{-N}$ and $\text{NO}_2\text{-N}$ increased from 43 to 82 $\mu\text{mol/L}$ ($P = 0.03$) and 13 to 17 $\mu\text{mol/L}$ ($P = 0.03$). In the low-tide period, the sluices were opened and a large amount of upstream effluent was discharged into the tidal creek wherein the concentrations of $\text{NH}_4\text{-N}$, $\text{NO}_3\text{-N}$, and $\text{NO}_2\text{-N}$ increased up to 212, 161, and 30 $\mu\text{mol/L}$, respectively (Figure 4a). $\delta^{15}\text{N-NO}_3^-$ increased from 6.6‰–9.0‰ during ebb tide to 9.9‰–22.3‰ in the effluent affected period ($P = 0.01$; Figure 4b). $\delta^{15}\text{N-NH}_4^+$ decreased gradually during ebb tide ($P = 0.06$) but fluctuated to a higher level in the effluent affected period. $\delta^{15}\text{N-N}_2\text{O}$ decreased from –0.8‰ to –3.2‰ ($P = 0.03$) during ebb tide with a slight fluctuation in the effluent affected period, while $\delta^{18}\text{O-N}_2\text{O}$ increased from 48.9‰ to 51.1‰ during ebb tide ($P = 0.03$). ΔN_2 and $\Delta\text{N}_2\text{O}$ showed an increasing trend ($P = 0.03$ for N_2 and $P = 0.02$ for N_2O) during measurement period (Figure 4c).

The plot of $\delta^{18}\text{O-NO}_3^-$ versus $\delta^{15}\text{N-NO}_3^-$ suggested the major sources of nitrate nitrogen (Figure 5). $\delta^{15}\text{N-NO}_3^-$ and $\delta^{18}\text{O-NO}_3^-$ values during ebb tide mostly fall within the range of soil organic nitrogen, before shifting to within the range of manure and sewage in the effluent affected period (low tide). In addition, a majority of measured ratios of $\delta^{15}\text{N}$ to $\delta^{18}\text{O}$ in

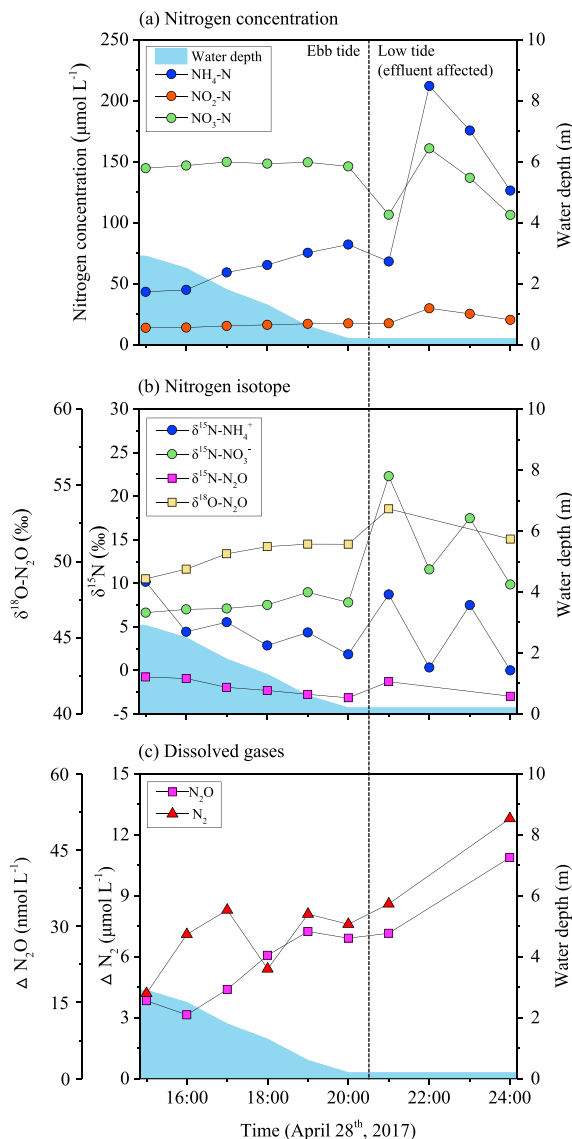


Figure 4. Temporal variation of nitrogen (a), isotopic compositions (b), and dissolved gases (c) in tidal creek (site T) during ebb tide and low tide when sluices open to discharge effluents. ΔN_2 and ΔN_2O indicate the difference between measured concentrations and equilibrium values with the atmosphere (refer to equations (1) and (2)).

4. Discussion

4.1. Hydrological Controls on Inorganic Nitrogen Exchange Between Mangroves and Estuary

Despite that in other mangrove systems particulate nitrogen can be an important pool of nitrogen (Valiela et al., 2018), this study is only focusing on dissolved inorganic forms. Here we emphasize discussion on inorganic nitrogen since DIN (and not DON) is the major form of dissolved nitrogen (Table 1).

Our results show that mangrove system served as a source of ammonium but a sink of nitrate to the estuary in most cases. The fact that NH_4-N concentrations were higher in the tidal creek than the estuary while NO_3-N concentrations were lower (except for October; Table 1) implies a net export of ammonium from mangroves through the tidal creek to adjacent estuary. In contrast, nitrate was likely imported from estuary to mangroves. The dominant controls on this exchange were processes within the sediments (discussed below). This nitrogen exchange between mangroves and estuary was mainly driven by tidal pumping. Ammonium export was more likely to occur during ebb tide rather than flood tide. NH_4-N in ebb tide

in June (Figure 6b). POC and TN varied little with depth. POC content ranged between 10 and 15 g/kg, and the TN content ranged between 1.0 and 1.5 g/kg (Figures 6c and 6d).

Nutrient concentrations in sediment pore water varied with depth (Figure 6). NH_4-N was relatively low in the top 10 cm ($<160 \mu\text{mol/L}$) but quickly increased to over $300 \mu\text{mol/L}$ in deeper sediments (Figure 6h). Depth-integrated concentration of NH_4-N in April ($380 \pm 335 \mu\text{mol/L}$) was much higher than in June ($209 \pm 148 \mu\text{mol/L}$; $P = 0.03$), and NH_4-N in December ($262 \pm 200 \mu\text{mol/L}$) was slightly lower than in June ($P = 0.24$). NO_3-N and NO_2-N in pore water were relatively low compared with NH_4-N and peaked at a depth of about 5–10 cm (Figures 6i and 6j). The colored dissolved organic matter (CDOM) in June was lower than in December; it was evenly distributed in June but increased with depth in December before declining again below 40 cm (Figure 6e). The concentration of DOC decreased, while DIC increased with depth (Figures 6f and 6g). It seems that most parameters had a turning point below 40 cm (mangrove root zone; Figure 6).

The functional gene abundance of nitrifiers and denitrifiers both exhibited a decreasing trend with depth (Table 2). The abundance of nitrous oxide reductase gene *nosZ* (2.30×10^7 – 8.79×10^8 copies per gram of dry soil) was far greater than nitrifiers gene AOB (1.24×10^6 – 9.55×10^7 copies per gram of dry soil) and AOA (6.39×10^6 copies per gram of dry soil). The abundance of *hzsB* (functional gene of anammox) in middle sediments was higher than in surface and bottom sediments but was much lower (8.62×10^5 – 1.82×10^6 copies per gram of dry soil) than nitrifiers gene overall.

3.4. Change of Nitrogen and Gases Production From Sediment Incubation

The reduction or increase of nitrogen and gaseous production in overlying water after 60-hr incubation varied with depth (Figure 7). NO_3-N and NO_2-N reduced at all depths, while NH_4-N increased significantly below 10 cm (Figure 7a). Compared with initial values, DIN reduced by 11%–23% in the upper 30 cm, while it started to increase below 30 cm as a result of high NH_4-N addition (Figure 7b). POC decreased by 6%–23%, and the maximum reduction occurred in the top sediments (5–10 cm; Figure 7b). N_2O production could only be detected in the upper 10-cm sediments. The production of N_2 was 0.8–1.3 $\mu\text{mol/g}$ showing a slight increase in deeper sediments.

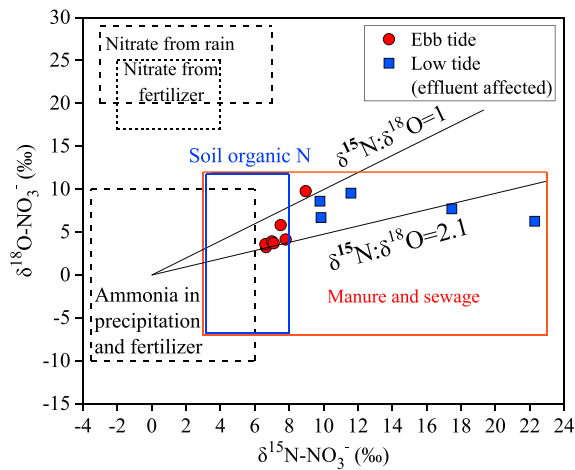


Figure 5. Identification of nitrate nitrogen sources according to isotopic compositions. Samples collected in tidal creek at site T during ebb tide and low tide (28 April 2017). Typical ranges of $\delta^{18}\text{O}$ and $\delta^{15}\text{N}$ values of nitrate from various sources were described by Kendall (1998).

was higher than flood tide (Table 1 and Figure 2). Positive correlations between the offset of $\text{NH}_4\text{-N}$, $\text{NO}_3\text{-N}$, DIN, and tidal range (Figure 3) confirmed the hydrological controls on inorganic nitrogen exchange between mangroves and estuary. One exception is the lower offset in June when the measurement was conducted after a major rainstorm event.

The studied mangrove forest was affected directly by external human perturbation, receiving the effluent of aquaculture ponds and wastewater when sluices were opened during low tide. High $\text{NH}_4\text{-N}$ and low $\text{NO}_3\text{-N}$ concentrations in effluent (Table 1) also contributed the offset of $\text{NH}_4\text{-N}$ and $\text{NO}_3\text{-N}$ in the tidal creek from the estuary. The $\text{NH}_4\text{-N}$ fraction (10%–28% of DIN) at mangrove and estuary sites was much lower than the effluent (59%), and the $\text{NO}_3\text{-N}$ fraction (44%–87% of DIN) was greater than the effluent (27%). Moreover, nitrate isotopic compositions across the ebb tide to low tide identified the changing sources with tidal state (Figures 4 and 5). $\delta^{15}\text{N-NO}_3^-$ was slightly increased, while $\delta^{15}\text{N-NH}_4^+$ decreased gradually during ebb tide, suggesting the mixing of mangrove sediment pore water where nitrogen cycling occurred (see more discussion below). In the low tide, $\delta^{15}\text{N-NO}_3^-$ and $\delta^{15}\text{N-NH}_4^+$ increased to a higher level (Figure 4), indicating a significant input of sluice effluents

containing human and/or animal wastes. In addition, nutrient concentration and isotope seem fluctuated in a different way, largely ascribing to the mixing of effluents from various sites through sluices along the dike (Figure 1 and Table S1). The time series measurement of nitrogen species and multi-isotopes confirmed that the timing of nitrogen export from mangroves to estuary was mainly driven by source supply and tidal pumping.

4.2. Biogeochemical Controls on Nitrogen Cycling in Mangrove Sediments

Mangrove sediments can store a large amount of organic carbon originating from mangrove plants, coastal water, or terrestrial inputs (Donato et al., 2011; Feller et al., 2003; Twilley et al., 1992). Mineralization of

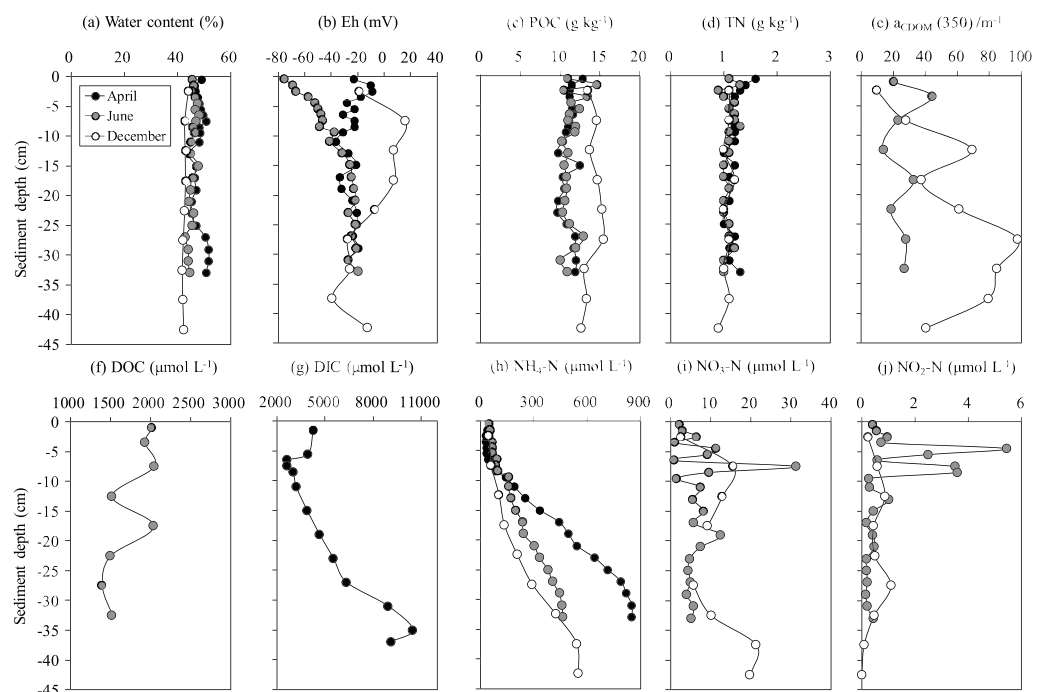


Figure 6. Concentrations of nutrient (h)–(j), DOC (f), DIC (g), and CDOM (e) in sediment pore water and physiochemical parameters (a)–(d) for different seasons in 2017.

Table 2
Functional Gene Abundance in Sediment Core and Pore Water Nutrient

Depth (cm)	AOA (copies per gram)	AOB (copies per gram)	nosZ (copies per gram)	hzsB (copies per gram)	NH ₄ -N (μmol/L)	NO ₃ -N (μmol/L)	NO ₂ -N (μmol/L)
0.5	6.39×10^6	9.55×10^7	8.79×10^8	8.62×10^5	49.6	2.3	0.4
19	Ct > 35*	2.45×10^6	4.53×10^7	1.82×10^6	241.4	12.6	0.4
33	2.61×10^5	1.24×10^6	2.30×10^7	1.19×10^6	465.0	5.2	0.4

Note. Sediment core for AOA, AOB, and nosZ was collected in June 2017. Sediment core for hzsB was collected in December 2017. Ct > 35 means that the abundance of AOA was below the detection limit.

organic matter (ammonification) likely resulted in large net NH₄-N accumulation in sediment pore water (Figure 6). NH₄-N can be nitrified in surface sediments and in sediments where there are open (oxygenated) burrows (common phenomenon in mangrove sediments), but in deeper sediments nitrification is inhibited due to anaerobic and reductive conditions (Eh < 0). The net increase in NH₄-N by the end of incubation implied that mineralization prevails over nitrification processes over depths greater than 10 cm (Figure 7). In addition, dissimilatory nitrate reduction to ammonium (DNRA) could also contribute to NH₄-N accumulation (Cao et al., 2016; Fernandes et al., 2012). The importance of DNRA was not explicitly evaluated here but was expected to be minor since availability of nitrite and nitrate in pore water was relatively low. Another process that could be occurring was the oxidation of ammonia by anaerobic ammonium oxidation (anammox). The gene abundance of hzsB (The anammox gene; 8.62×10^5 – 1.82×10^6 copies per gram of dry soil; Table 2) detected in the sediment profile was 2 orders lower than nosZ denitrification gene abundance (2.30×10^7 – 8.79×10^8 copies per gram of dry soil; Table 2). This result was similar to a recent study on mangrove sediments, which also suggests that denitrification rather than anammox dominates nitrate loss (Cao et al., 2017). We concluded that strong mineralization and limited nitrification resulted in an accumulation of NH₄-N in mangrove sediments (10–40 cm).

It was observed that while NH₄-N concentration increased in the creek water during ebb tide, δ¹⁵N-NH₄⁺ decreased. This is the period of the tidal cycle when it is expected that nutrients would be outfluxed from sediment into the creek. Given the anthropogenic sources input and within-creek nitrification resulting in δ¹⁵N-NH₄⁺, a lower δ¹⁵N-NH₄⁺ is likely a result of mineralization of soil organic matter. This isotope message confirmed that the mangrove sediments is the major source of ammonia in the creek.

In contrast to the high levels of NH₄-N in sediment pore water, nitrate concentration was fairly low (most less than 30 μmol/L, Figure 6i) but not zero as would be expected for a purely anoxic system. The presence of nitrate in the pore waters is likely due to the presence of large open (crab) burrows. Several biogeochemical processes can contribute to nitrate removal. NO₃-N can be reduced to N₂ (N₂O) via denitrification (incomplete denitrification) and cause increase in δ¹⁵N-NO₃⁻ (Xue et al., 2009). In this study, we indeed observed a slight increase in δ¹⁵N-NO₃⁻ (Figure 4b) and excess dissolved N₂ and N₂O in creek water during ebb tide (Figure 4c). As noted above the anammox gene was 2 orders of magnitude less than the denitrifiers gene (Table 2), suggesting that anammox was relatively unimportant. Furthermore, the ratio of δ¹⁵N to δ¹⁸O in NO₃⁻ fell into the ratio range (1.0–2.1), reflecting the occurrence of denitrification (Figure 5). These findings indicate that denitrification plays an important role in nitrate removal within mangrove sediments. Further evidence for this conclusion comes from the incubation experiment where we found an overall reduction of NO₃-N and production of N₂ regardless of depth (Figure 7). Theoretically, two mole NO₃-N will produce one mole N₂ by denitrification, but the change in NO₃-N was far less than the production of N₂ (NO₃-N_{loss}: N₂_{pro} = 0.5–1.2); this likely reflects the fact that nitrification occurred at the early stage of incubation to make up the nitrate removal.

Our data also show that the mangrove sediments is an important source of N₂O. Pore water NH₄-N in surface sediments was fairly low and NO₃-N peaked at a depth of 5–10 cm (Figure 6h and 6i), indicating that nitrification mainly occurs in surface sediments. Eh in top sediments was low, especially the minimum value observed in June (Figure 6b), a result which can be largely ascribed to oxygen consumption associated with higher microorganism respiration in summer (Giblin et al., 2013). The much higher abundance of nitrifiers (AOA and AOB) in the upper sediments than the deep sediments (Table 2), together with the fact that N₂O

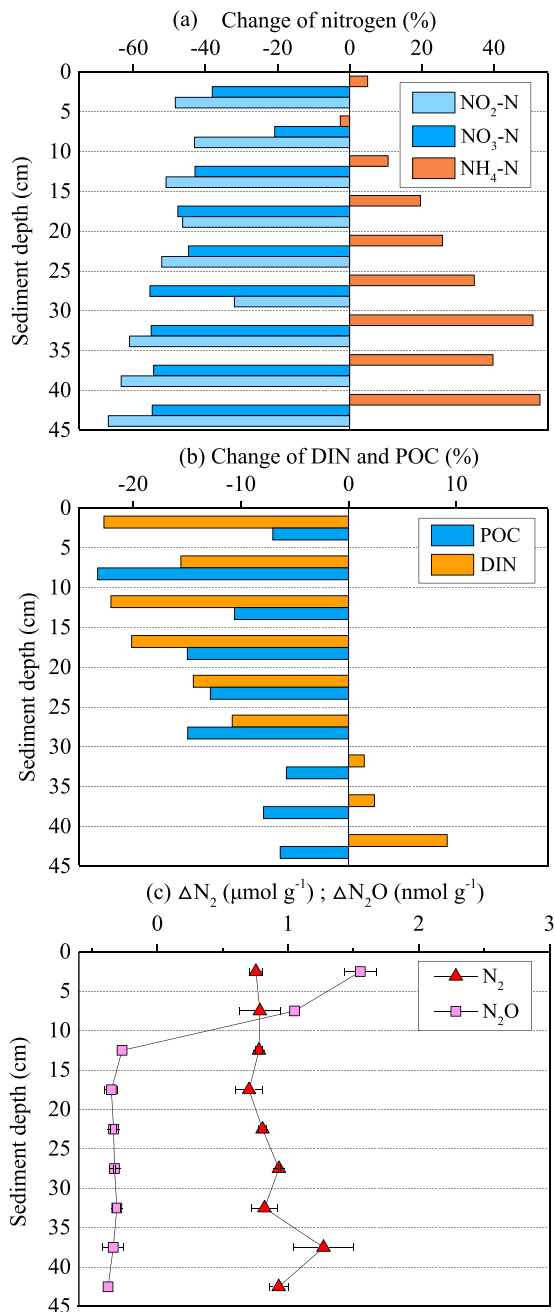


Figure 7. Change in nutrient (a and b), POC (b), and production of dissolved gases (c) after 60-hr sediment incubation. Positive values mean production and negative values mean reduction after incubation. Error bars indicate one standard deviation from mean of triplicates. ΔN_2 and $\Delta\text{N}_2\text{O}$ indicate the difference between measured concentrations and equilibrium values with the atmosphere (refer to equations 1 and 2).

was only produced in the upper 10-cm sediments during incubation (Figure 7), further confirmed the occurrence of nitrification mainly in surface sediments. Previous studies reported that AOB may outnumber AOA in the ammonium-oxidizing area (Damashek et al., 2015). AOB abundance had a good positive correlation with potential nitrification rate, while the relationship between AOA abundance and potential rate was much weaker (Damashek et al., 2015; Smith et al., 2015). Therefore, nitrification and heterotrophic respiration occurring in the top oxic sediments and tidal creek water might contribute to the excess N_2O emission.

Numerous studies have suggested that both nitrification (Barnes et al., 2006; Muñozhincapié et al., 2002) and denitrification (Allen et al., 2007; Lee et al., 2008) contribute to N_2O production. Unlike pristine mangrove, creek waters are a sink of nitrous oxide (Maher et al., 2016); our results showed that N_2O concentration was oversaturated and $\Delta\text{N}_2\text{O}$ increased from 23 to 36 nmol/L during ebb tide (Figure 4c). A good correlation between N_2 and N_2O could be obtained by incomplete denitrification (Yan et al., 2012). Unfortunately, we found a weak correlation ($r = 0.48$, $P > 0.05$) during ebb tide. We examined major processes involved in N_2O production by comparing the observed $\delta^{15}\text{N}$ and $\delta^{18}\text{O}$ of N_2O with the expected values for different processes following the method reported in Thuan et al. (2018). Both $\delta^{15}\text{N}$ and $\delta^{18}\text{O}$ fell within or were very close to the expected range of incomplete denitrification (Figure S2). This suggested that following within-sediment denitrification, the majority of dissolved N_2O was transported to the tidal creek via subsurface runoff. The ratio of $\delta^{15}\text{N}$ to $\delta^{18}\text{O}$ should be stable if there are no other sources, but it slightly decreased from -0.02 to -0.06 in ebb tide (Figure S2). Given that the expected $\delta^{15}\text{N}:\delta^{18}\text{O}$ ratio of N_2O from nitrification is lower than denitrification (Thuan et al., 2018), and the high potential nitrification likely occurred in mangrove tidal creek (Xiao et al., 2018), we speculated that nitrification of surface runoff and pore water ammonium after it reached the tidal creek also contributed to N_2O formation and outgassing.

4.3. Seasonality of Nitrogen Exchange

The net DIN offset switched between seasons (Figure 3c), showing that the mangrove system acted as a source of DIN in spring and winter and a net sink in summer and fall. Outfluxing of DIN from the mangrove system occurs only when nutrient availability exceeds demand by mangrove trees and the associated microbial communities (Dittmar & Lara, 2001b). Increased temperature, solar radiation, and rainfall in summer and fall (Figure S1) might increase nutrient cycling and primary production (Andrews et al., 2000; Hoque et al., 2010; Janssens et al., 2001). Litter production has been suggested to elevate the productivity of forest. Study showed that litterfall (which is high in carbon but low in DIN) was influenced by air temperature, and increased with increases in air temperature from spring to early summer, and reached a maximum in fall (Chen et al., 2009). It has been suggested that this leads to higher nutrient uptake in summer and fall. In June and October, the mangrove acted as a

net sink of DIN (Figure 2). This was also the period of highest temperature and thus highest microbial denitrification rate. By contrast, nutrient uptake is reduced in winter and spring when both the mangroves and the sedimentary microbial community are less active (lower temperatures).

Rainfall can influence this seasonal cycle. In this region there is a wet summer-fall season and a relatively dry winter-spring. The rainfall will influence the watershed nitrogen loading to the estuary by wet deposition and river runoff. There was no obvious seasonal trends for $\text{NH}_4\text{-N}$ and $\text{NO}_3\text{-N}$ concentrations in rainwater

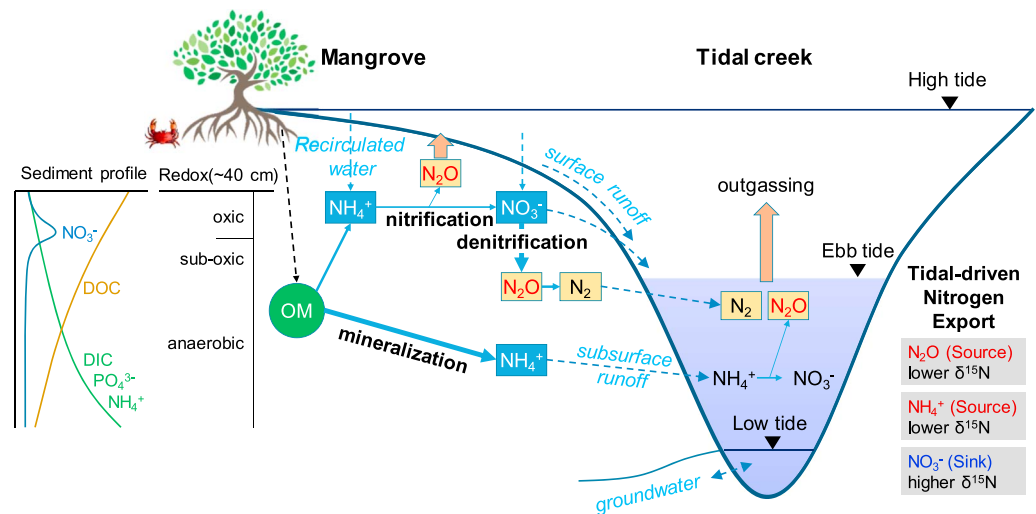


Figure 8. A conceptual schematic of hydrobiogeochemical controls on nitrogen cycling, lateral transport, and greenhouse gases outgassing in the mangrove-creek interfaces.

around the study region (Wu et al., 2018). However, the majority of rainfall occurred in summer especially in June (395 mm) and August (404 mm; Figure S1). $\text{NH}_4\text{-N}$ measured in the tidal creek in June was the lowest (Figure 2). This was sampled just after a major rainfall event, and this low value was likely resulting from dilution by the increased rainfall and river discharge. $\text{NO}_3\text{-N}$ in estuarine water was relative stable over seasons (Figure 2). Nitrate offset was generally negative, but very different in April, when its concentration in tidal creek was higher than the estuary (Figure 2). $\text{NH}_4\text{-N}$ in April was the largest in both sediment pore water (Figure 6) and in tidal creek among all measurements (Table 1), suggesting that this was the peak of net nitrification. This addition of nitrate through enhanced nitrification once large $\text{NH}_4\text{-N}$ was released from sediment pore water into tidal creek seems to occur preferentially during ebb tide.

Current results indicate the importance of mangrove-tidal creek interface to the nutrients exchange between mangrove and the marine system. The study also provides a first glimpse into the major controls on mangrove nitrogen cycling and outwelling. However, it is a complex system. The spatial and temporal variation of nitrogen forms (Figures 2 and 6) is a combined result of tidal driven exchange, climate factors, microbe-driven cycling, and bio-uptake. The linkages among major elements (carbon, nitrogen, phosphorus, sulfur, and iron) and processes regulating their roles in blue carbon remain to be quantified, particularly under increasing human and climate perturbation. Further research is needed to understand in more detail the balance of the biogeochemical processes across the mangrove sediment-creek-estuary continuum.

5. Conclusions

A conceptual schematic of hydrobiogeochemical controls on nitrogen lateral transport between mangrove and tidal creek is illustrated in Figure 8. Mangrove sediment system was found to mostly serve as a source of $\text{NH}_4\text{-N}$ but a sink of $\text{NO}_3\text{-N}$ in relation to the adjacent estuary. The offset of nitrogen concentrations in creek water from the estuary was found to correlate with tidal range. Overall, there was a net export of DIN from mangroves in winter and spring but a net import to mangroves in summer and fall, mainly driven by tidal pumping, associated hydrological processes (recirculated water flow, surface runoff, subsurface runoff, and ground water) and seasonal patterns. $\text{NH}_4\text{-N}$ was enriched in sediment pore water and increased with depth (10–40 cm), likely resulting from strong ammonification with limited nitrification in anaerobic conditions. In contrast, denitrification played a vital role in nitrate removal while producing N_2 , while anaerobic ammonium oxidation was shown to have a lesser role. Evidence for this statement, included the low nitrate level in pore water, nitrate reduction after sediment incubation with abundant functional gene (*nosZ*), and increasing $\delta^{15}\text{N-NO}_3^-$ in ebb tide. Isotope signatures suggested that the majority of N_2O was derived from incomplete denitrification within sediments, but a large potential nitrification of pore water ammonium also

contributed to N₂O formation, which is a major greenhouse gas. To sum up, the sediment-tidal creek interface plays a key role in the nitrogen lateral transport between the mangrove system and coastal water. Strong mineralization and denitrification in mangrove sediments are major processes shaping mangroves as an ammonium source, nitrate sink, and hotspot for greenhouse gases outgassing.

Acknowledgments

This research was supported by the Key Laboratory of the Coastal and Wetland Ecosystems (WELRI201601), the State Key Laboratory of Marine Environmental Science (MELRI1603), and the Fundamental Research Funds for the Central Universities of China (20720180118). We thank Nan Ling, Xinjuan Gao, Dan Yu, Peiliang Dai, Xinyu Zhang, Lei Liu, Kadija Kane, Jie Wang, and Taotao Cao, Xiuwen Ji for their help with field works and lab analysis. We thank Xudong Zhu for providing meteorological data recorded by an eddy covariance tower in study site. We thank Professor Jack Middelburg and Professor Robert Aller for their insightful comments. Special thanks to Professor Michael Krom for his assistance with English and other editing, which was done while in receipt of a visiting Professorship at Xiamen University. Data can be obtained in supporting information. The authors declare that they have no conflict of interest.

References

- Allen, D. E., Dalal, R. C., Rennenberg, H., Meyer, R. L., Reeves, S., & Schmidt, S. (2007). Spatial and temporal variation of nitrous oxide and methane flux between subtropical mangrove sediments and the atmosphere. *Soil Biology & Biochemistry*, *39*(2), 622–631. <https://doi.org/10.1016/j.soilbio.2006.09.013>
- Alongi, D. M. (2015). The impact of climate change on mangrove forests. *Current Climate Change Reports*, *1*(1), 30–39.
- Amano, T., Yoshinaga, I., Yamagishi, T., Chu, V. T., Pham, T. T., Ueda, S., et al. (2011). Contribution of anammox bacteria to benthic nitrogen cycling in a mangrove forest and shrimp ponds, Haiphong, Vietnam. *Microbes and Environments*, *26*(1), 1–6. <https://doi.org/10.1264/jsm.2011.0150>
- Amberger, A., & Schmidt, H. L. (1987). Natürliche Isotopengehalte von Nitrat als Indikatoren für dessen Herkunft. *Geochimica Et Cosmochimica Acta*, *51*(10), 2699–2705.
- Andrews, J. A., Matamala, R., Westover, K. M., & Schlesinger, W. H. (2000). Temperature effects on the diversity of soil heterotrophs and the delta ¹³C of soil-respired CO₂. *Soil Biology & Biochemistry*, *32*(5), 699–706. [https://doi.org/10.1016/S0038-0717\(99\)00206-0](https://doi.org/10.1016/S0038-0717(99)00206-0)
- Barnes, J., Ramesh, R., Purvaja, R., Rajkumar, A. N., Kumar, B. S., Krithika, K., et al. (2006). Tidal dynamics and rainfall control N₂O and CH₄ emissions from a pristine mangrove creek. *Geophysical Research Letters*, *33*, L15405. <https://doi.org/10.1029/2006GL026829>
- Cao, W. Z., Guan, Q. S., Li, Y., Wang, M., & Liu, B. L. (2017). The contribution of denitrification and anaerobic ammonium oxidation to N₂ production in mangrove sediments in Southeast China. *Journal of Soils and Sediments*, *17*(6), 1767–1776. <https://doi.org/10.1007/s11368-017-1653-0>
- Cao, W. Z., Yang, J. X., Li, Y., Liu, B. L., Wang, F. F., & Chang, C. T. (2016). Dissimilatory nitrate reduction to ammonium conserves nitrogen in anthropogenically affected subtropical mangrove sediments in Southeast China. *Marine Pollution Bulletin*, *110*(1), 155–161. <https://doi.org/10.1016/j.marpolbul.2016.06.068>
- Casciotti, K. L., Sigman, D. M., Hastings, M. G., Bohlke, J. K., & Hilkert, A. (2002). Measurement of the oxygen isotopic composition of nitrate in seawater and freshwater using the denitrifier method. *Analytical Chemistry*, *74*(19), 4905–4912. <https://doi.org/10.1021/ac020113w>
- Chen, L. Z., Zan, Q. J., Li, M. G., Shen, J. Y., & Liao, W. B. (2009). Litter dynamics and forest structure of the introduced *Sonneratia caseolaris* mangrove forest in Shenzhen, China. *Estuarine Coastal and Shelf Science*, *85*(2), 241–246. <https://doi.org/10.1016/j.ecss.2009.08.007>
- Chen, N. W., Wu, J., Chen, Z., Lu, T., & Wang, L. (2014). Spatial-temporal variation of dissolved N₂ and denitrification in an agricultural river network, southeast China. *Agriculture Ecosystems & Environment*, *189*, 1–10. <https://doi.org/10.1016/j.agee.2014.03.004>
- Chen, N. W., Wu, J. Z., Zhou, X. P., Chen, Z. H., & Lu, T. (2015). Riverine N₂O production, emissions and export from a region dominated by agriculture in Southeast Asia (Jiulong River). *Agriculture Ecosystems & Environment*, *208*, 37–47. <https://doi.org/10.1016/j.agee.2015.04.024>
- Chen, R. H., & Twilley, R. R. (1999). Patterns of mangrove forest structure and soil nutrient dynamics along the Shark River estuary, Florida. *Estuaries*, *22*(4), 955–970. <https://doi.org/10.2307/1353075>
- Damashek, J., Smith, J. M., Mosier, A. C., & Francis, C. A. (2015). Benthic ammonia oxidizers differ in community structure and biogeochemical potential across a riverine delta. *Frontiers in Microbiology*, *5*, 743.
- Dittmar, T. (1999). Nutrient dynamics in a mangrove creek (North Brazil) during the dry season. *Mangroves & Salt Marshes*, *3*(3), 185–195.
- Dittmar, T., & Lara, R. J. (2001a). Do mangroves rather than rivers provide nutrients to coastal environments south of the Amazon River? Evidence from long-term flux measurements. *Marine Ecology Progress Series*, *213*(4), 67–77.
- Dittmar, T., & Lara, R. J. (2001b). Driving forces behind nutrient and organic matter dynamics in a mangrove tidal creek in North Brazil. *Estuarine Coastal and Shelf Science*, *52*(2), 249–259. <https://doi.org/10.1006/ecss.2000.0743>
- Donato, D. C., Kauffman, J. B., Murdiyarto, D., Kurnianto, S., Stidham, M., & Kanninen, M. (2011). Mangroves among the most carbon-rich forests in the tropics. *Nature Geoscience*, *4*(5), 293–297.
- Feller, I. C., Lovelock, C. E., Berger, U., McKee, K. L., Joye, S. B., & Ball, M. C. (2010). Biocomplexity in mangrove ecosystems. *Annual Review of Marine Science*, *2*, 395–417. <https://doi.org/10.1146/annurev.marine.010908.163809>
- Feller, I. C., McKee, K. L., Whigham, D. F., & O'Neill, J. P. (2003). Nitrogen vs. phosphorus limitation across an ecotonal gradient in a mangrove forest. *Biogeochemistry*, *62*(2), 145–175.
- Fernandes, S. O., Bonin, P. C., Michotey, V. D., Garcia, N., & Lokabharathi, P. A. (2012). Nitrogen-limited mangrove ecosystems conserve N through dissimilatory nitrate reduction to ammonium. *Scientific Reports*, *2*(5), 419.
- Francis, C. A., Roberts, K. J., Beman, J. M., Santoro, A. E., & Oakley, B. B. (2005). Ubiquity and diversity of ammonia-oxidizing archaea in water columns and sediments of the ocean. *Proceedings of the National Academy of Sciences of the United States of America*, *102*(41), 14,683–14,688.
- Giblin, A. E., Tobias, C. R., Song, B., Weston, N., Banta, G. T., & Rivera-Monroy, V. H. (2013). The importance of dissimilatory nitrate reduction to ammonium (DNRA) in the nitrogen cycle of coastal ecosystems. *Oceanography*, *26*(3), 124–131. <https://doi.org/10.5670/oceanog.2013.54>
- Gilman, E. L., Ellison, J., Duke, N. C., & Field, C. (2008). Threats to mangroves from climate change and adaptation options: A review. *Aquatic Botany*, *89*(2), 237–250. <https://doi.org/10.1016/j.aquabot.2007.12.009>
- Guo, W., Yang, L., Zhai, W., Chen, W., Osburn, C. L., Huang, X., & Li, Y. (2014). Runoff-mediated seasonal oscillation in the dynamics of dissolved organic matter in different branches of a large bifurcated estuary-The Changjiang Estuary. *Journal of Geophysical Research: Biogeosciences*, *119*, 776–793. <https://doi.org/10.1002/2013JG002540>
- Holmes, R. M., McClelland, J. W., Sigman, D. M., Fry, B., & Peterson, B. J. (1998). Measuring ¹⁵N-NH₄⁺ in marine, estuarine and fresh waters: An adaptation of the ammonia diffusion method for samples with low ammonium concentrations. *Marine Chemistry*, *60*(3–4), 235–243. [https://doi.org/10.1016/S0304-4203\(97\)00099-6](https://doi.org/10.1016/S0304-4203(97)00099-6)
- Hoque, A. T. M. R., Sharma, S., Suwa, R., Mori, S., & Hagihara, A. (2010). Seasonal variation in the size-dependent respiration of mangroves *Kandelia obovata*. *Marine Ecology Progress Series*, *404*(12), 31–37.

- Inoue, T., Nohara, S., Takagi, H., & Anzai, Y. (2011). Contrast of nitrogen contents around roots of mangrove plants. *Plant and Soil*, 339(1-2), 471–483. <https://doi.org/10.1007/s11104-010-0604-y>
- Janssens, I. A., Lankreijer, H., Matteucci, G., Kowalski, A. S., Buchmann, N., Epron, D., et al. (2001). Productivity overshadows temperature in determining soil and ecosystem respiration across European forests. *Global Change Biology*, 7(3), 269–278. <https://doi.org/10.1046/j.1365-2486.2001.00412.x>
- Kendall, C. (1998). Tracing nitrogen sources and cycling in catchments. In *Isotope tracers in Catchment Hydrology* (pp. 519–576). <https://doi.org/10.1016/b978-0-444-81546-0.50023-9>
- Kristensen, E., Jensen, M. H., Banta, G. T., Hansen, K., Holmer, M., & King, G. M. (1998). Transformation and transport of inorganic nitrogen in sediments of a Southeast Asian mangrove forest. *Aquatic Microbial Ecology*, 15(2), 165–175. <https://doi.org/10.3354/ame015165>
- Lee, R. Y., Porubsky, W. P., Feller, I. C., McKee, K. L., & Joye, S. B. (2008). Porewater biogeochemistry and soil metabolism in dwarf red mangrove habitats (Twin Cays, Belize). *Biogeochemistry*, 87(2), 181–198. <https://doi.org/10.1007/s10533-008-9176-9>
- Li, M., & Gu, J. D. (2013). Community structure and transcript responses of anammox bacteria, AOA, and AOB in mangrove sediment microcosms amended with ammonium and nitrite. *Applied Microbiology and Biotechnology*, 97(22), 9859–9874. <https://doi.org/10.1007/s00253-012-4683-y>
- Lovelock, C. E., Ball, M. C., Martin, K. C., & Feller, I. C. (2009). Nutrient enrichment increases mortality of mangroves. *Plos One*, 4(5), 4. <https://doi.org/10.1371/journal.pone.0005600>
- Maher, D. T., Sippo, J. Z., Tait, D. R., Holloway, C., & Santos, I. R. (2016). Pristine mangrove creek waters are a sink of nitrous oxide. *Scientific Reports*, 6, 1–8. <https://doi.org/10.1038/srep25701>
- Mandal, S., Ray, S., & Ghosh, P. B. (2013). Impact of mangrove litterfall on nitrogen dynamics of virgin and reclaimed islands of Sundarban mangrove ecosystem, India. *Ecological Modelling*, 252, 153–166. <https://doi.org/10.1016/j.ecolmodel.2012.06.038>
- McLeod, E., Chmura, G. L., Bouillon, S., Salm, R., Bjork, M., Duarte, C. M., et al. (2011). A blueprint for blue carbon: Toward an improved understanding of the role of vegetated coastal habitats in sequestering CO₂. *Frontiers in Ecology and the Environment*, 9(10), 552–560. <https://doi.org/10.1890/110004>
- Muñozhincapié, M., Morell, J. M., & Corredor, J. E. J. M. P. B. (2002). Increase of nitrous oxide flux to the atmosphere upon nitrogen addition to red mangrove sediments. *Marine Pollution Bulletin*, 44(10), 992–996.
- Reef, R., Feller, I. C., & Lovelock, C. E. (2010). Nutrition of mangroves. *Tree Physiology*, 30(9), 1148–1160.
- Reis, C. R. G., Nardoto, G. B., & Oliveira, R. S. (2017). Global overview on nitrogen dynamics in mangroves and consequences of increasing nitrogen availability for these systems. *Plant and Soil*, 410(1-2), 1–19. <https://doi.org/10.1007/s11104-016-3123-7>
- Rivera-Monroy, V. H., Day, J. W., Twilley, R. R., Vera-Herrera, F., & Coronado-Molina, C. (1995). Flux of nitrogen and sediment in a fringe mangrove forest in Terminos Lagoon, Mexico. *Estuarine Coastal & Shelf Science*, 40(2), 139–160.
- Rivera-Monroy, V. H., Lee, S. Y., Kristensen, E., & Twilley, R. R. (2017). *Mangrove ecosystems: A global biogeographic perspective*. Springer.
- Rivera-Monroy, V. H., & Twilley, R. R. (1996). The relative role of denitrification and immobilization in the fate of inorganic nitrogen in mangrove sediments (Terminos Lagoon, Mexico). *Limnology and Oceanography*, 41(2), 284–296. <https://doi.org/10.4319/lo.1996.41.2.0284>
- Sadat-Noori, M., Santos, I. R., Tait, D. R., Reading, M. J., & Sanders, C. J. (2017). High porewater exchange in a mangrove-dominated estuary revealed from short-lived radium isotopes. *Journal of Hydrology*, 553, 188–198. <https://doi.org/10.1016/j.jhydrol.2017.07.058>
- Sánchez-Carrillo, S., Sánchez-Andrés, R., Alatorre, L. C., Angeler, D. G., Alvarez-Cobelas, M., & Arreola-Lizarraga, J. A. (2009). Nutrient fluxes in a semi-arid microtidal mangrove wetland in the Gulf of California. *Estuarine Coastal and Shelf Science*, 82(4), 654–662. <https://doi.org/10.1016/j.ecss.2009.03.002>
- Sanders, C. J., Eyre, B. D., Santos, I. R., Machado, W., Luiz-Silva, W., Smoak, J. M., et al. (2014). Elevated rates of organic carbon, nitrogen, and phosphorus accumulation in a highly impacted mangrove wetland. *Geophysical Research Letters*, 41, 2475–2480. <https://doi.org/10.1002/2014GL059789>
- Scala, D. J., & Kerkhof, L. J. (1999). Diversity of nitrous oxide reductase (nosZ) genes in continental shelf sediments. *Applied & Environmental Microbiology*, 65(4), 1681–1687.
- Sigman, D. M., Casciotti, K. L., Andreani, M., Barford, C., Galanter, M., & Bohlke, J. K. (2001). A bacterial method for the nitrogen isotopic analysis of nitrate in seawater and freshwater. *Analytical Chemistry*, 73(17), 4145–4153. <https://doi.org/10.1021/ac10088e>
- Smith, J. M., Mosier, A. C., & Francis, C. A. (2015). Spatiotemporal relationships between the abundance, distribution, and potential activities of ammonia-oxidizing and denitrifying microorganisms in intertidal sediments. *Microbial Ecology*, 69(1), 13–24.
- Thuan, N. C., Koba, K., Yano, M., Makabe, A., Kinh, C. T., Terada, A., et al. (2018). N₂O production by denitrification in an urban river: evidence from isotopes, functional genes, and dissolved organic matter. *Limnology*, 19(1), 115–126. <https://doi.org/10.1007/s10201-017-0524-0>
- Twilley, R. R., Chen, R. H., & Hargis, T. (1992). Carbon sinks in mangroves and their implications to carbon budget of tropical coastal ecosystems. *Water Air & Soil Pollution*, 64(1-2), 265–288.
- Valiela, I., Elmstrom, E., Lloret, J., Stone, T., & Camilli, L. (2018). Tropical land-sea couplings: Role of watershed deforestation, mangrove estuary processing, and marine inputs on N fluxes in coastal Pacific Panama. *Science of the Total Environment*, 630, 126–140. <https://doi.org/10.1016/j.scitotenv.2018.02.189>
- Wang, H. T., Su, J. Q., Zheng, T. L., & Yang, X. R. (2014). Impacts of vegetation, tidal process, and depth on the activities, abundances, and community compositions of denitrifiers in mangrove sediment. *Applied Microbiology and Biotechnology*, 98(22), 9375–9387. <https://doi.org/10.1007/s00253-014-6017-8>
- Wang, S., Wang, Y., Feng, X., Zhai, L., & Zhu, G. (2011). Quantitative analyses of ammonia-oxidizing archaea and bacteria in the sediments of four nitrogen-rich wetlands in China. *Applied Microbiology & Biotechnology*, 90(2), 779–787.
- Weiss, C., Weiss, J., Boy, J., Iskandar, I., Mikutta, R., & Guggenberger, G. (2016). Soil organic carbon stocks in estuarine and marine mangrove ecosystems are driven by nutrient colimitation of P and N. *Ecology and Evolution*, 6(14), 5043–5056. <https://doi.org/10.1002/ece3.2258>
- Weiss, R. F. (1970). The solubility of nitrogen, oxygen and argon in water and seawater. *Deep-Sea Research and Oceanographic Abstracts*, 17(4), 721–735.
- Weiss, R. F., & Price, B. A. (1980). Nitrous-oxide solubility in water and seawater. *Marine Chemistry*, 8(4), 347–359. [https://doi.org/10.1016/0304-4203\(80\)90024-9](https://doi.org/10.1016/0304-4203(80)90024-9)
- Wu, S. P., Dai, L. H., Wei, Y., Zhu, H., Zhang, Y. J., Schwab, J. J., & Yuan, C. S. (2018). Atmospheric ammonia measurements along the coastal lines of Southeastern China: Implications for inorganic nitrogen deposition to coastal waters. *Atmospheric Environment*, 177, 1–11. <https://doi.org/10.1016/j.atmosenv.2017.12.040>

- Xiao, K., Wu, J. P., Li, H. L., Hong, Y. G., Wilson, A. M., Jiao, J. J., & Shananan, M. (2018). Nitrogen fate in a subtropical mangrove swamp: Potential association with seawater-groundwater exchange. *Science of the Total Environment*, *635*, 586–597. <https://doi.org/10.1016/j.scitotenv.2018.04.143>
- Xue, D., Botte, J., De Baets, B., Accoe, F., Nestler, A., Taylor, P., et al. (2009). Present limitations and future prospects of stable isotope methods for nitrate source identification in surface- and groundwater. *Water Research*, *43*(5), 1159–1170. <https://doi.org/10.1016/j.watres.2008.12.048>
- Yan, W., Yang, L., Wang, F., Wang, J., & Ma, P. (2012). Riverine N₂O concentrations, exports to estuary and emissions to atmosphere from the Changjiang River in response to increasing nitrogen loads. *Global Biogeochemical Cycles*, *26*, GB4006. <https://doi.org/10.1029/2010GB003984>
- Zhou, H. C., Wei, S. D., Zeng, Q., Zhang, L. H., Tam, N. F. Y., & Lin, Y. M. (2010). Nutrient and caloric dynamics in *Avicennia marina* leaves at different developmental and decay stages in Zhangjiang River Estuary, China. *Estuarine Coastal and Shelf Science*, *87*(1), 21–26. <https://doi.org/10.1016/j.ecss.2009.12.005>